Journal of Materials Chemistry C

Accepted Manuscript

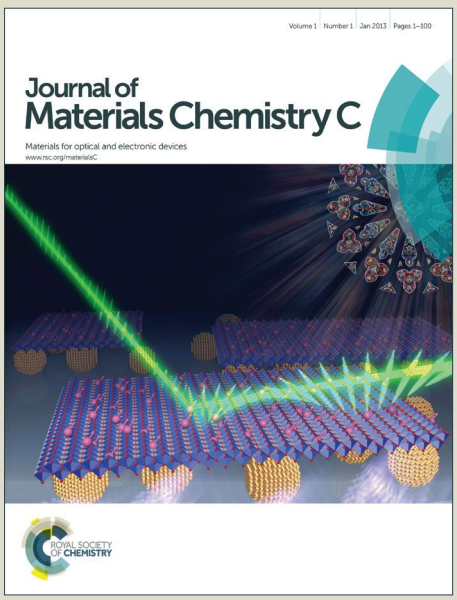

ROYAL SOCIETY OF CHEMISTRY

www.rsc.org/materialsC

Journal Name

ARTICLE

Salicylaldimine Difluoroboron Complexes Containing *tert*-Butyl Groups: Nontraditional π-Gelator and Piezofluorochromic Compounds

Received 00th January 20xx,
Accepted 00th January 20xx

DOI: 10.1039/x0xx00000x

www.rsc.org/

Peng Gong, Hao Yang, Jingbo Sun, Zhenqi Zhang, Jiabao Sun, Pengchong Xue, Ran Lu*

We have synthesized three new salicylaldimine difluoroboron complexes with *tert*-butyl groups **1B**-**3B**, which are high emissive in solutions and in solid states. It was found that salicylaldehydehydrazone difluoroboron complex **1B** could form organogels in *n*-hexane and the mixture of petroleum ether/CH_2Cl_2, and 1D nanoribbons with intense blue emission could be fabricated via the gelation of the nontraditional organogelator **1B** directed by balanced π-π interaction. However, the other two salicylaldimine difluoroboron complexes **2B** and **3B** with a spacer of benzene ring could not form gel due to strong π-π interaction, but exhibited piezofluorochromic behaviors. The as-prepared crystals of **2B** and **3B** giving blue-green fluorescence could be transformed into the powders emitting yellow light upon grinding, and the emission could recover when the ground powders were heated. It suggested that the reversible piezofluorochromism orignated from the transformation between crystalline and amorphous states. Therefore, it provided a strategy for designing new nontraditional π-gelators and piezofluorochromic materials via tuning π-π interaction.

Introduction

Recently, π-conjugated molecules containing heteroatoms, including N, S, P and B, have drawn great attention due to their unique optoelectrical properties[1] and practical applications in organic light-emitting diode,[2] organic field-effect transistor,[3] photovoltaic cell,[4] stimulus-responsive materials[5] and sensors.[6] Especially, the organic boron-containing π-conjugated molecules, such as difluoroboron complexes (N,N- O,O- and N,O-chelated boron complexes), are excellent fluorophores. Besides their high quantum yields in solutions as well as in solid states, large molar extinction coefficients, high electron affinities and sensitivity to the surrounding medium, difluoroboron complexes are used as building blocks in supramolecular assemblies,[7] in particular, in low molecular mass organogels. For example, the N,N-chelated boron complexes of BODIPY have been employed as functional materials in sensors,[8] solar cells[9] and near-infrared luminescence materials.[10] The O,O-chelated boron complexes have been found to exhibit self-assembling and fluorescence sensory properties.[11] Meanwhile, the emitting colors of some N,O-chelated boron complexes can be tuned by external mechanical forces due to the transformation of the molecular packing mode or molecular conformation, and these piezofluorochromic materials would have potential applications in mechano-sensors, security papers and data storage devices.[12] In our previous work, we have found that the difluoroboron complexes with steric hindrance moieties showed high-contrast piezofluorochromic properties and good gelation abilities.[11a-11b,13] Since the balanced π-π interaction played a key role in the molecular packing in aggregated states,[14] we have introduced *tert*-butyl into carbazole derivatives to tune the strength of π-π interaction and gained piezofluorochromic emitters and functional π-gels. However, to the best of our knowledge, the salicylaldimine difluoroboron complex has not been reported in organogel system as well as in piezofluorochromic material. With these in mind, herein, we synthesized three salicylaldimine difluoroboron complexes **1B-3B** with *tert*-butyl groups (Scheme 1). Only salicylaldehydehydrazone difluoroboron complex **1B** was found to be a gelator and self-assembled into 1D nanoribbons with strong emission in gel state. It should be noted that the traditional gelators usually contain H-bonded units (such as amide, amino acid or urea moieties) and auxiliary groups of long alkyl chain, sugar or cholesterol.[14a,15] Herein, the synthesis of nontraditional gelator **1B** without the above auxiliary groups would lead to atom economy and be helpful for the design of new nontraditional gelator. Moreover, the salicylaldimine difluoroboron complexes with a spacer of benzene ring **2B** and **3B** showed piezofluorochromic behaviors although they could not form gel in the selected solvents. For example, the as-prepared crystals of **2B** and **3B** exhibited blue-green fluorescence and could be transformed into the ground powders emitting yellow light upon grinding. When the ground powders were heated or fumed with organic solvent, the

State Key Laboratory of Supramolecular Structure and Materials, College of Chemistry, Jilin University, Changchun 130012, P. R. China
E-mail: luran@mail.jlu.edu.cn
Electronic Supplementary Information (ESI) available: [Analytical data and spectra (^{1}H and ^{13}C NMR), mass spectrometry data, DFT calculation of configuration optimization materials]. See DOI: 10.1039/x0xx00000x

emission could recover. The XRD patterns of **2B** and **3B** in different solid stated illustrated that the reversible piezofluorochromism was resulted from the transformation between crystalline and amorphous states. Therefore, the introduction of *tert*-butyl would lead to loose packing of difluoroboron complexes in aggregated states, and be favorable for yielding nontraditional π-gelator as well as piezofluorochromic compounds. This work would provide strategy for the design of new functional organic materials.

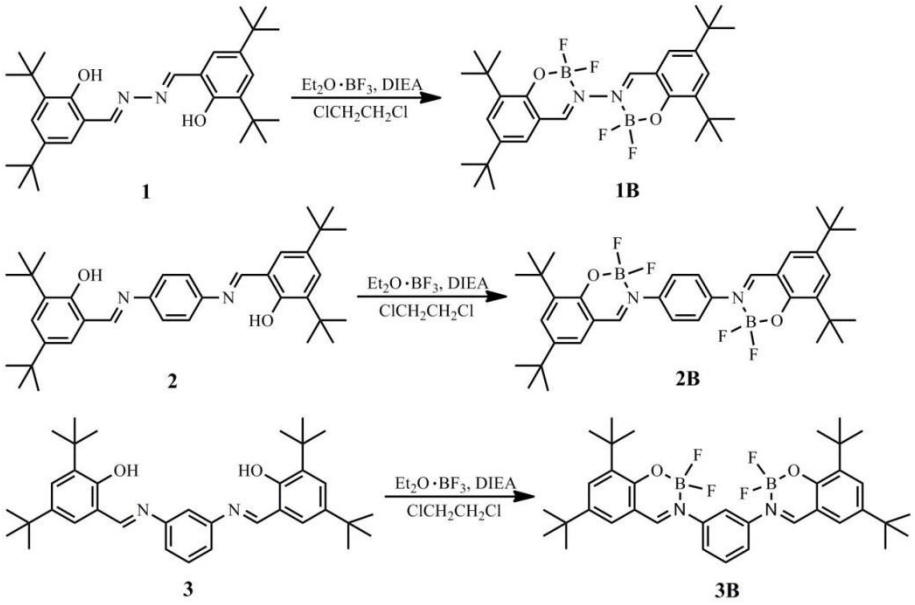

Scheme 1. Synthetic routes for salicylaldimine difluoroboron complexes **1B**-**3B**.

Results and discussion

Synthesis

Scheme 1 shows the synthetic routes for salicylaldimine difluoroboron complexes **1B-3B**. Firstly, the ligands of salicylaldimine **1**-**3** were synthesized according to the reported procedures.[16] The reaction of compound **1** with $Et_2O{\cdot}BF_3$ was carried out under N_2 atmosphere in 1,2-dichloroethane using N,N-diisopropylethylamine as a base to afford **1B** in a low yield of 11%. On the contrary, the reaction of **2** or **3** with $Et_2O{\cdot}BF_3$ gave difluoroboron complexes **2B** or **3B** in a high yield of 83% or 90%, respectively. The reason for the lower yield of compound **1B** than the other difluoroboron complexes might be that the strong electron-withdrawing ability of the first formed difluoroboron complex moiety would weaken the coordinating ability of the second free salicylaldimine in the mono-chelated difluoroboron complex formed from compound **1** since the two salicylaldimine units were linked directly via N-N bond. In the cases of compounds **2** and **3**, the two salicylaldimine units showed good reactivity with BF_3 because they were separated by a spacer of benzene ring. The target molecules were characterized by ^{1}H NMR, ^{13}C NMR, FT-IR and MALDI-TOF mass spectrometry.

UV-vis absorption and fluorescence emission spectra in solutions

The UV-vis absorption and fluorescence emission spectra of **1B-3B** in CH_2Cl_2 (5.0×10^{-6} M) were shown in Figure 1, and the data were listed in Table S1. The absorption bands of **1B**

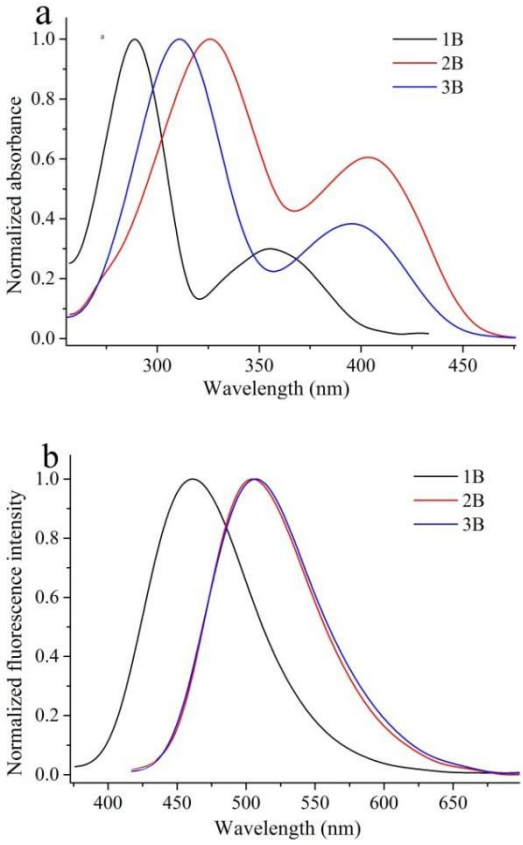

Figure 1. Normalized a) UV-vis absorption and b) fluorescence emission spectra of **1B**-**3B** in CH_2Cl_2 (5.0×10^{-6} M), the excited wavelength for **1B**-**3B** were 355 nm, 400 nm and 400 nm, respectively.

showed two absorption peaks at 289 and 355 nm, and **2B** and **3B** exhibited red-shifted absorption bands compared with **1B**, respectively. For example, **2B** showed strong absorption at 326 nm and 403 nm and **3B** gave strong absorption located at 311 nm and 396 nm. The reason why the absorption of **1B** appeared in high-energy region compared with **2B** and **3B** was that the twisted molecular conformation of **1B** led to the poor conjugation (Figure S1). Meanwhile, we found that the absorption bands in long wavelength for **2B** (403 nm) exhibited a red-shift compared with that for **3B** (396 nm) on account of the large conjugation degree. As shown in Figure 1b, **1B-3B** gave strong emission centered at 458 nm, 505 nm and 506 nm, respectively, and their fluorescence quantum yields were 19% (using quinine sulfate in 0.1 M H_2SO_4 as standard, Φ_F = 54.6%), 13% and 19% (using 9,10-diphenylanthracene in benzene as the standard, Φ_F = 85%), respectively, in CH_2Cl_2. Similarly, the emission of **1B** also emerged in high-energy region compared with **2B** and **3B** due to its limited conjugation. It was noticed that the emission spectra of **2B** and **3B** were quite similar in CH_2Cl_2 although their conjugated degree was different. Similar electronic spectral behaviors of **2B** and **3B** were observed in other solvents. As shown in Figure S2, red-shifts of the absorption bands for **2B** compared with **3B** could also be detected in toluene, THF and DMF due to the large conjugated degree of **2B**. The emission spectra of **2B** and **3B** were quite similar in the above solvents. As a result, we found that the Stokes shifts of **3B** (5301 cm^{-1} in toluene, 5880 cm^{-1} in THF and 5987 cm^{-1} in DMF) were larger than **2B** (4612 cm^{-1} in toluene, 5195 cm^{-1} in THF and 5507 cm^{-1} in DMF) in the above solvents, which meant that the excited state of **3B** underwent larger conformational change than **2B**. Therefore, we deemed that the large conjugated degree and the small Stokes shift of **2B** compared with **3B** led to their similar emission spectra.

Gelation properties

The gelation abilities **1B-3B** were investigated in the selected method.[17] As shown in Table 1, only compound **1B** could form opaque gels in *n*-hexane and petroleum ether/CH_2Cl_2 (v/v = 25/7) under ultrasound stimulus.[18] The critical gelation concentration (CGC) for **1B** was 5.1 mM and 7.25 mM, respectively, in *n*-hexane and petroleum ether/CH_2Cl_2 (v/v = 25/7). The obtained gels were stable for several months at room temperature and could be destroyed upon heated. If the hot solution was stimulated by ultrasound again, the organogel could be reformed after ageing. To understand the different gelation abilities of the three compounds, their molecular configurations were shown in Figure S1. According to the optimized configurations for **1B** calculated by the DFT method (B3LYP/6-31G level) on Gaussian 09 software, **1B** gave a nonplanar conformation (Figure S1a). Such nonplanar aromatic unit and the large steric effect *tert*-butyl groups would decrease the strength of π-π interaction and afford balanced π-π interaction to induce the gel formation. Although the conjugated skeletons of **2B** and **3B** showed nonplanar configuration (Figure S1b and S1c), no gel was formed due to their enhanced conjugation. The morphology of xerogel **1B** obtained from petroleum ether/CH_2Cl_2 (v/v 25/7) was investigated by optical microscope, fluorescence microscope and SEM. As shown in Figure 2, gelator **1B** self-assembled into long nanoribbons with diameters of 0.4-1.2 μm, which emitted strong blue light, in gel state. The Φ_F of xerogel **1B** was 13% (Table S1), meaning emissive 1D nanomaterials could be gained via the gelation of salicylaldimine difluoroboron complexes. In order to investigate the driving forces for the gel formation, the UV-vis absorption spectra of **1B** in dilute solution and in xerogel were given in Figure 3a. It was found that the absorption peak at 355 nm for **1B** in CH_2Cl_2 blue-shifted to 350 nm in xerogel, which demonstrated the formation of *H*-aggregates.[19] Meanwhile, we found that the emission intensity at 453 nm for compound **1B** decreased during the gelation process (Figure 3b), suggesting that π-π interaction played a

Table 1 Gelation abilities of compounds **1B-3B** in organic solvents.

Solvent	**1B** (CGC[a]/mM)	**2B**	**3B**
Methanol	P	P	P
Ethanol	P	P	P
CH_2Cl_2	S	S	S
1,2-Dichloroethane	S	S	S
DMF	S	S	S
DMSO	S	S	S
Cyclohexane	PG	P	P
n-Hexane	G (5.1)	P	P
Petroleum ether	P	P	P
Petroleum ether/ CH_2Cl_2 (v/v=25/7)	G (7.25)	P	P

P: precipitate; PG: partly gel; S: soluble; G: gel.
[a] CGC: critical gelation concentration.

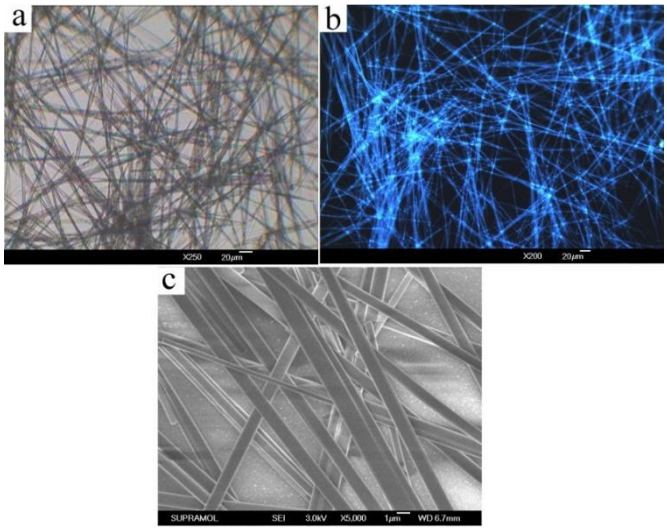

Figure 2. (a) Optical microscope, (b) fluorescence microscope (λ_{ex} = 365 nm) and (c) SEM images of xerogel **1B** obtained from petroleum ether/CH_2Cl_2 (v/v 25/7).

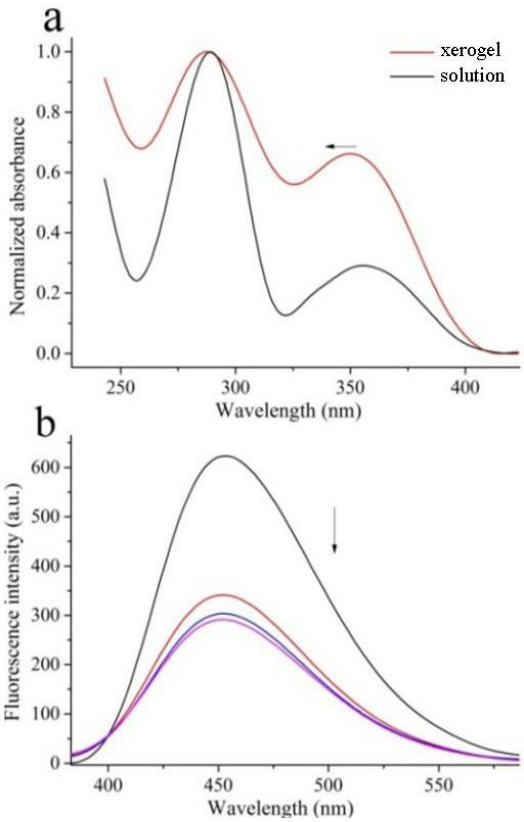

Figure 3. (a) UV-vis absorption spectra of **1B** in CH_2Cl_2 (5.0×10^{-6} M) and in xerogel film and (b) fluorescence emission spectra of **1B** during the gelation process in petroleum ether/CH_2Cl_2 (v/v = 25/7) excited at 365 nm.

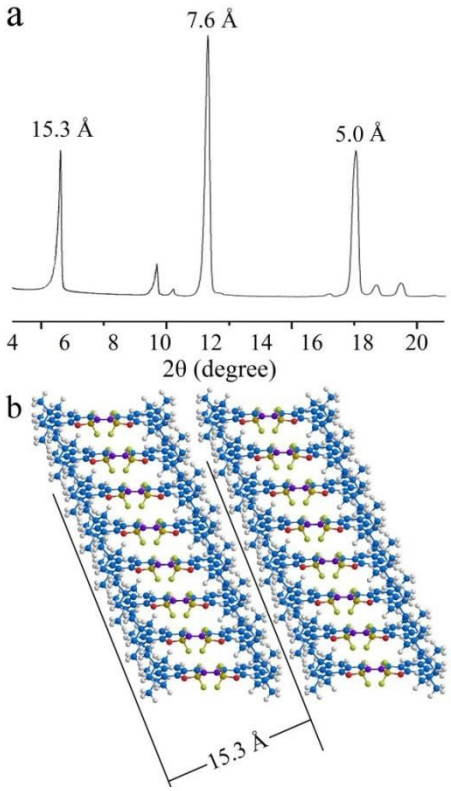

Figure 4. (a) XRD pattern of xerogel **1B** and (b) the proposed molecular packing model of **1B** in gel phase.

role in the gel formation. The XRD pattern of xerogel 1B was shown in Figure 4a, and we found three strong diffraction peaks with *d*-spacing of 15.3, 7.6 and 5.0 Å, respectively, corresponding to a ratio of ca. 1: 1/2: 1/3. It indicated that a layered structure with a long period of 15.3 Å was generated, which was quite similar to the optimized molecular length of compound 1B (15.4 Å, Figure S1a).[20] Therefore, we proposed the molecular packing model of 1B in gel state as shown in Figure 4b, and *H*-aggregates were involved.

Piezofluorochromism

We investigated the piezofluorochromic properties of the three compounds and found that **2B** and **3B** gave different emitting behaviors upon the treatment of grinding and fuming. As shown in Figure 5a, **2B** emitted strong blue-green fluorescence centered at ca. 487 nm in the as-prepared crystal, which changed into yellow emitting powder (ca. 509 nm) upon ground. The Φ_F of **2B** in as-prepared crystal and in ground powder was same (12%, Table S1). In addition, the emitting color of **2B** in ground powder could recover to blue-green by heating instead of solvent fuming, and the changes of emission were reversible.[21] If the heated powder of **2B** was reground, its fluorescence red-shifted to 508 nm again. The influence of heating temperature and time was investigated. As the ground powder of **2B** was heated at 100 °C for 1 min, the emission showed slight change (Figure S3). If the heating time was prolonged to 30 min, the fluorescence peak blue-shifted from 509 nm to 493 nm. When the ground powder was heated at 200 °C for 10 min, the emission shifted to 478 nm.[22] Similarly, compound **3B** gave blue-green emission (480 nm) with Φ_F of 17% in as-prepared crystal and yellow emission (503 nm) with Φ_F of 16% in ground powder (Figure 5b). However, the ground powder **3B** could turn into blue-green emitting sample via fuming with CH_2Cl_2 except for heating due to its better solubility in CH_2Cl_2 than **2B**. However, after **3B** was heated at 200 °C for 2 min, its fluorescence peak could shift to 476 nm. It meant that the recovery of the emitting color from yellow to blue-green was easier for the ground powder **3B** than **2B**. It might originate from the weaker π-π interaction between **3B** than **2B** in solid states. We could see that the fluorescence emission red-shifted to 508 nm again after the heated or fumed powders of **3B** were reground. Thus, the piezofluorochromism of **3B** was also reversible. Meanwhile, the UV-vis absorption spectra of **2B** and **3B** in different solid states were given in Figure S4 to reveal the piezofluorochromic mechanism. From Figure S4a we could see three absorption peaks at 226 nm, 333 nm and 415 nm for **2B** in as-prepared crystal. After ground, the absorption of **2B** blue-shifted to 224 nm, 328 nm and 407 nm, respectively, which might be resulted from the changes of molecular packing modes.[23] The absorption spectral changes of **3B** in different solid states were similar to those of **2B**.

In order to investigate the phase transition during piezofluorochromic processes, XRD patterns of **2B** in different solid states were shown in Figure 6. The as-prepared crystal **2B**

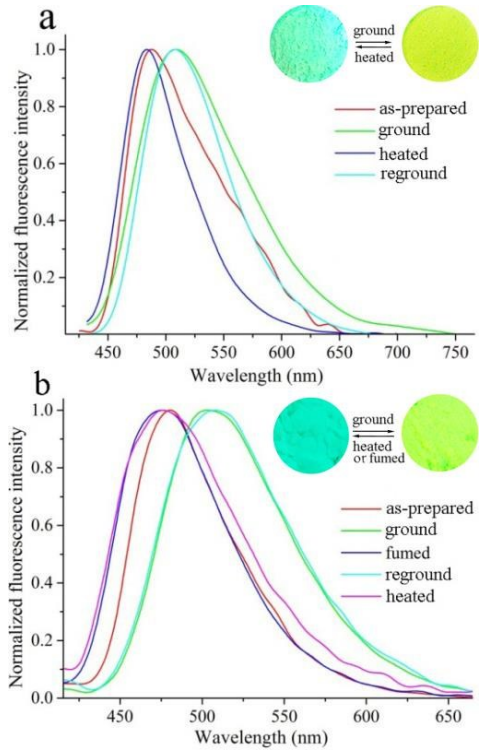

Figure 5. Fluorescence emission spectra of **2B** (a) and **3B** (b) excited at 350 nm in different solid states; Insets: photos of **2B** and **3B** in different solid states irradiated at 365 nm.

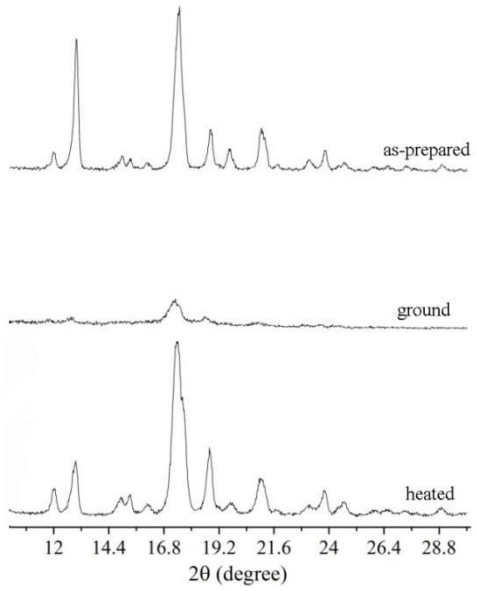

Figure 6. XRD patterns of compound **2B** in different solid states.

exhibited several sharp and intense diffraction peaks, which disappeared when it was ground, revealing a transformation from crystalline structure to an amorphous state.[24] Meanwhile, the diffraction peaks could be recovered if the ground powder was heated. The XRD patterns of **3B** in different solid states showed similar results (Figure S5). It suggested that the reversible changes of the emitting colors for **2B** and **3B** in response to grinding/heating treatment was originating from the transformation between crystalline and amorphous states, which could be further proved by the DSC curves of **2B** and **3B** in different states (Figure S6). One exothermic transition peak was detected at 164.0 °C or 206.0 °C for **2B** or **3B** in ground powder, and might be ascribed to the cold-crystallization (crystallizing from glass state) of ground sample upon annealing.[25] It illustrated that the amorphous state was a metastable one.

Conclusions

In summary, three new salicylaldimine difluoroboron complexes with *tert*-butyl groups **1B-3B** were synthesized and their photophysical, self-assembling and piezofluorochromic properties were investigated. It was found that only salicylaldehydehydrazone difluoroboron complex **1B** could form organogels in *n*-hexane and petroleum ether/CH_2Cl_2 (v/v = 25/7) under ultrasound stimulus. We deemed that the nonplanar aromatic unit and the large steric effect *tert*-butyl groups in **1B** would lead to balanced π-π interaction and induce the gel formation. The other two salicylaldimine difluoroboron complexes **2B** and **3B** could not gelate the selected solvents due to the strong π-π interaction. It is worth noting that as a nontraditional organogelator, **1B** could self-assemble into 1D nanoribbons with intense blue emission. On the other hand, **2B** and **3B** showed reversible piezofluorochromism. The as-prepared crystals of **2B** and **3B** emitted strong blue-green light and could be transformed into the powders emitting yellow light after grinding, and the fluorescence could recover when the ground powders were heated or fumed with organic solvent. It was found that the reversible changes of the emitting colors for **2B** and **3B** induced by grinding and heating/fuming was resulted from the transformation between crystalline and amorphous states. It provided the strategy for designing new nontraditional π-gelators and piezofluorochromic materials via tuning π-π interaction.

Experimental section

General information

^{1}H NMR spectra were recorded with Bruker avance III 400 MHz by using $CDCl_3$ as the solvent. ^{13}C NMR spectra were recorded on a mercury plus 100 MHz using $CDCl_3$ as the solvent. Mass spectra were performed on Agilent 1100 MS series and AXIMA CFR MALDI/TOF (Matrix assisted laser desorption ionization/Time-of-flight) MS (COMPACT). FT-IR spectrum was measured with a Nicolet-360 FT-IR spectrometer by incorporation of sample in KBr disk. UV-vis absorption spectra were determined on a Shimadzu UV-1601PC Spectrophotometer. Fluorescence emission spectra were carried out on a Shimadzu RF-5301 Luminescence Spectrometer. The fluorescence quantum yields of **1B** in CH_2Cl_2 were measured using quinine sulfate in 0.1 H_2SO_4, and those for **2B** and **3B** in CH_2Cl_2 were measured using 9,10-diphenylanthracene in benzene as the standard. The solid fluorescence quantum yields of **1B**-**3B** were measured using

Edinburgh Instrument FLS920. Fluorescence microscopy image was obtained on a fluorescence microscope (Olympus Reflected Fluorescence System BX51, Olympus, Japan). Scanning electron microscope (SEM) image was obtained on JEOL JSM-6700F (operating at 5 kV). The optical microscope image was obtained on JNOEC XS-201. XRD pattern of xerogel was determined on the PANalytical-Empyrean and the XRD patterns of **2B** and **3B** in different solid states were determined on Rigaku-SmartLab (III). DSC measurements were taken by NETZSCH STA499F3 QMS403D \ Bruker V70. The optimized configurations were calculated by the DFT (B3LYP/6-31G) method on Gaussian 09 software.[26]

Synthesis

All solvents and reagents were used as received. The salicylaldimine **1**-**3** were synthesized according to previously reported procedures.[16]

6,6',8,8'-tetra-*tert*-butyl-2,2,2',2'-tetrafluoro-2*H*,2'*H*-2λ^4,2'λ^4,3λ^4,3'λ^4-3,3'-bibenzo[*e*][1,3,2]oxazaborinine (**1B**)
Compound **1** (5.0 g, 10.76 mmol) and DIEA (18.8 ml, 23.69 mmol) were dissolved in dry 1,2-dichloroethane (180 mL) and the solution was refluxed for 10 min under N_2 atmosphere. Then, $BF_3{\cdot}Et_2O$ (24.8 mL, 193.68 mmol) were added dropwise and the mixture was refluxed for 14 h. The solvent was removed under vacuum. The residual solids were purified by column chromatography using butanone/petroleum ether(v/v= 1/5) as eluent, followed by recrystallization from CH_2Cl_2/petroleum ether, to afford **1B** (650 mg, 11%) as white floccule. m.p. = 175.0-177.0 °C. ^{1}H NMR (400 MHz, $CDCl_3$) δ 8.15 (s, 2H), 7.61 (d, J = 2.4 Hz, 2H), 7.12 (d, J = 2.4 Hz, 2H), 1.45 (s, 18H), 1.30 (s, 18H) (Figure S7). ^{13}C NMR (100 MHz, $CDCl_3$) δ 154.13, 153.82, 142.47, 138.90, 131.65, 124.33, 114.27, 35.16, 34.28, 31.28, 29.3 (Figure S8). MS, m/z: cal.: 560.3, found: 560.3, $[M]^+$ (Figure S9). FT-IR (KBr, cm^{-1}): 3393, 3318, 3003, 2955, 2870, 1646, 1626, 1517, 1476, 1392, 1363, 1314, 1284, 1249, 1151, 1123, 1060, 928, 898, 810, 770, 718, 647, 617, 549, 517.

1,4-bis(6,8-di-*tert*-butyl-2,2-difluoro-2*H*-2λ^4,3λ^4-benzo[*e*][1,3,2]oxazaborinin-3-yl)benzene (**2B**)
By following the synthetic procedure for **1B**, **2B** was synthesized from compound **2** (2.0 g, 3.70 mmol) and $BF_3{\cdot}Et_2O$ (2.57 mL, 20.04 mmol). The crude product was purified by column chromatography using CH_2Cl_2 as eluent, yielding **2B** (1.95 g, 83%) as a yellow green solid. m.p. = 407 °C (obtained from DSC). ^{1}H NMR (400 MHz, $CDCl_3$) δ 8.44 (s, 2H), 7.77 (d, J = 2.4 Hz, 2H), 7.69 (s, 4H), 7.31 (d, J = 2.4 Hz, 2H), 1.50 (s, 18H), 1.34 (s, 18H) (Figure S10). ^{13}C NMR (100 MHz, $CDCl_3$) δ 164.35, 157.52, 142.88, 142.72, 139.68, 135.16, 126.22, 124.89, 115.63, 35.26, 34.38, 31.17, 29.31 (Figure S11). MS, m/z: cal.: 636.4, found: 638.0 $[M+H]^+$ (Figure S12). IR (KBr, cm^{-1}): 3057, 2961, 2872, 1621, 1567, 1505, 1473, 1411, 1392, 1364, 1348, 1310, 1285, 1262, 1248, 1214, 1151, 1064, 1031, 993, 928, 879, 843, 807, 775, 684, 643, 615, 560, 534.

1,3-bis(6,8-di-*tert*-butyl-2,2-difluoro-2*H*-2λ^4,3λ^4-benzo[*e*][1,3,2]oxazaborinin-3-yl)benzene (3B)
By following the synthetic procedure for **1B**, **3B** was synthesized from compound **3** (1.0 g, 1.85 mmol) and $BF_3{\cdot}Et_2O$ (1.28 mL, 10.00 mmol). The crude product was purified by column chromatography using CH_2Cl_2 as eluent, yielding **3B** (1.06 g, 90% as a yellow green solid. m.p. = 353.0 °C (obtained from DSC). ^{1}H NMR (400 MHz, $CDCl_3$) δ 8.48 (s, 2H), 7.77 (d, J = 2.4 Hz, 2H), 7.70-7.61 (m, 4H), 7.32 (d, J = 2.4 Hz, 2H), 1.50 (s, 18H), 1.33 (s, 18H) (Figure S13). ^{13}C NMR (100 MHz, $CDCl_3$) δ 164.86, 157.46, 143.40, 142.91, 139.52, 135.21, 130.86, 126.50, 124.13, 118.81, 115.64, 35.24, 34.38, 31.17, 29.32 (Figure S14). MS, m/z: cal.: 636.4, found: 637.2 $[M+H]^+$ (Figure S15). IR (KBr, cm^{-1}): 3077, 2961, 2870, 1629, 1601, 1566, 1471, 1444, 1393, 1363, 1345, 1312, 1287, 1259, 1243, 1192, 1135, 1058, 1007, 986, 938, 893, 832, 793, 776, 758, 696, 643, 609, 575, 549, 530, 443.

Acknowledgements

This work was financially supported by the National Natural Science Foundation of China (21374041) and the Open Project of State Key Laboratory of Supramolecular Structure and Materials (SKLSSM2015014).

Notes and references

1 (a) J. L. Li, A. C. Grimsdale. *Chem. Soc. Rev*., 2010, **39**, 2399-2410; (b) S. Durben, T. Baumgartner. *Angew. Chem. Int. Ed*., 2011, **50**, 7948-7952; (c) M. Mao, M. G. Ren, Q. H. Song. *Chem. Eur. J*., 2012, **18**, 15512-15522; (d) M. Huong Ha-Thi, V. Souchon, A. Hamdi, R. Métivier, V. Alain, K. Nakatani, P. G. Lacroix, J. Pierre Genét, V. Michelet, I. Leray. *Chem. Eur. J*., **12**, 9056-9065; (e)W. Li, Q. D. Li, C. H. Duan, S. J. Liu, L. Ying, F. Huang, Y. Cao. *Dyes Pigments*., 2015, **113**, 1-7; (f)X. Lefèvre, F. Moggia, O. Segut, Y. P. Lin, Y. Ksari, G. Delafosse, K. Smaali, D. GuèRin, V. Derycke, D. Vuillaume, S. Lenfant, L. Patrone, B. Jousselme. *J. Phys. Chem. C.*, 2015, **119**, 5703-5713; (g) M. Gilbert, B. Albinsson. *Chem. Soc. Rev*., 2015, **44**, 845-862; (h) Y. Ren, W. H. Kan, V. Thangadurai, T. Baumgartner. *Angew. Chem. Int. Ed*., 2012, **51**, 3964-3968; (i) G. Zhang, J. Chen, S. J. Payne, S. E. Kooi, J. N. Demas, C. L. Fraser. *J. Am. Chem. Soc.*, 2007, **129**, 8942-8943; (j) H. Chong, H. A. Lin, M. Y. Shen, C. Y. Liu, H. C. Zhao, H. H. Yu. *Org. Lett*., 2015.DOI: 10.1021/acs.orglett.5b00875

2 (a) M. Romain, S. Thiery, A. Shirinskaya, C. Declairieux, D. Tondelier, B. Geffroy, O. Jeannin, J. R. Berthelot, R. Métivier, C. Poriel. *Angew. Chem. Int. Ed.,* 2015, **54**, 1176-1180; (b) H. Chen, W. Delaunay, J. Li, Z. Y. Wang, P. A. Bouit, D. Tondelier, B. Geffroy. F. Mathey, Z. Duan, R. Réau, M. Hissler. *Org. Lett*., 2013, **15**, 330-333; (c) L. Y. Bian, J. F. Hai, E. W. Zhu, J. S. Yu, Y. Liu, J. Zhou, G. D. Ge, W. H. Tang. *J. Mater. Chem. A*., 2015, **3**, 1920-1924; (d) A. Thangthong, N. Prachumrak, S. Saengsuwan, S. Namuangruk, T. Keawin, S. Jungsuttiwong, T. Sudyoadsuka, V. Promarak. *J. Mater. Chem. C.*, 2015, **3**, 3081-3086.

3 (a) A. Facchetti. *A.Mater. Today*., 2007, **10**, 28-37; (b) W. K. Zhong, J. Xu, S. Sun, J. F. Liang, B. Zhang, R. F. He, L. F. Lan, F. Huang, L. Ying, W. Yang, J. B. Peng, Y. Cao. *Org. Electron*., 2015, **23**, 17-27; (c) B. Y. Fu, C. Y. Wang, B. D. Rose, Y. D. Jiang, M. Chang, P. H. Chu, Z. B. Yuan, C. Fuentes-Hernandez,

B. Kippelen, J. L. Brédas, D. M. Collard, E. Reichmanis. *Chem. Mater*., 2015, **27**, 2928-2937.
4 (a) A. Facchetti. *Chem. Mater*., 2011, **23**, 733-758; (b) J. L. Wang, Z. Wu, J. S. Miao, K. K. Liu, Z. F. Chang, R. B. Zhang, H. B. Wu, Y. Cao. *Chem. Mater.,* 2015, **27**, 4338-4348; (c) J. L. Wang, Q. R. Yin, J. S. Miao, Z. Wu, Z. F. Chang, Y. Cao, R. B. Zhang, J. Y. Wang, H. B. Wu , Y. Cao. *Adv. Funct. Mater.,* 2015, **25**, 3514-3523.
5 H. Chen, Y. Feng, G. J. Deng, Z. X. Liu, Y. M. He, Q. H. Fan. *Chem. Eur. J.,* 2015, **21**, 1-11.
6 (a) L. Zang, Y. K. Che, J. S. Moore. *Acc. Chem. Res.,* 2008, **41**, 1596-1608; (b) A. Bamesberger, G. Kim, J. Woo, H. S. Cao. *J Fluoresc*., 2015, **25**, 25-29; (c) P. Q. Leng, F. L. Zhao, B.C. Yin, B.C. Ye. *Chem. Commun.*, 2015, **51**, 8712-8714; (d) M. Shamsipur, M. A. Tabrizi, M. Mahkam, J. Aboudi. *Electroanalysis*., 2015, **27**, 1466-1472.
7 (a) O. Altintas, D. Schulze-Suenninghausen, B. Luy, C. Barner-Kowollik. *Eur. Polym. J.*, 2015, **62**, 409-417; (b) G. Echue, G. C. Lloyd-Jones, C. F. J. Faul. *Chem. Eur. J.,* 2015, **21**, 5118-5128; (c) F. Cheng, W. M. Wan, Y. Zhou, X. L. Sun, E. M. Bonderd, F. Jäkle. *Polym. Chem.,* 2015, **6**, 4650-4656.
8 (a) N. Sakamoto, C. Ikeda, M. Yamamura, T. Nabeshim. *Chem. Commun.*, 2012, **48**, 4818-4820; (b) S. Erbas-Cakmak, E. U. Akkaya, *Org. Lett*., 2014, **16**, 2946-2949.
9 (a) Y. Kubo, D. Eguchi, As. Matsumoto, R. Nishiyabu, H. Yakushiji, K. Shigaki, M. Kaneko. *J. Mater. Chem. A.*, 2014, **2**, 5204-5211; (b) A. Bessette, G. S. Hanan. *Chem. Soc. Rev*., 2014, **43**, 3342-3405.
10 (a) T. Sarma, P. K. Panda, J. I. Setsune. *Chem. Commun*., 2013, **49**, 9806-9808; (b) G. Ulrich, S. Goeb, A. D. Nicola, P. Retailleau, R. Ziessel. *J. Org. Chem.*, 2011, **76**, 4489-4505.
11 (a) X. L. Liu, X. F. Zhang, R. Lu, P. C. Xue, D. F. Xu, H. P. Zhou. *J. Mater. Chem*., 2011, **21**, 8756-8765; (b) X. F. Zhang, R. Lu, J. H. Jia, X. L. Liu, P. C. Xue, D. F. Xu, H. P. Zhou. *Chem. Commun.*, 2010, **46**, 8419-8421; (c) C. Qian, K. Y. Cao, X. L. Liu, X. F. Zhang, D. F. Xu, P. C. Xue, R. Lu. *Chinese Sci. Bull*., 2012, **57**, 4264-4271; (d) C. Qian, G. H. Hong, M. Y. Liu, P. C. Xue, R. Lu. *Tetrahedron.*, 2014, **70**, 3935-3942.
12 (a) Z. Q. Zhang, P. C. Xue, P. Gong, G. H. Zhang, J. Peng, R. Lu. *J. Mater. Chem. C.*, 2014, **2**, 9543-9551; (b) Z. G. Chi, X.Q. Zhang, B. J. Xu, X. Zhou, C. P. Ma, Y. Zhang, S. W. Liua, J. R. Xu. *Chem. Soc. Rev*., 2012, **41**, 3878-3896; (c) P. C. Xue, P. Chen, J.H. Jia, Q.X. Xu, J.B. Sun, B.Q. Yao, Z.Q. Zhang, R. Lu. *Chem. Commun.,* 2014, **50**, 2569-2571; (d) G. F. Zhang, M. P. Aldred, Z. Q. Chen, T. Chen, X. G. Meng, M. Q. Zhu. *RSC Adv.,* 2015, **5**, 1079-1082; (e) Q. K. Qi, J. Y. Qian, X. Tan, J. B. Zhang, L. J. Wang, B. Xu, B. Zou, W. J. Tian. *Adv. Funct. Mater.,* 2015,DOI: 10.1002/adfm.201501224.
13 (a) X. C. Yang, R. Lu, T. H. Xu, P. C. Xue, X. L. Liu, Y. Y. Zhao. *Chem. Commun.,* 2008, 453-455; (b) Y. Bando, T. Sakurai, S. Seki, H. Maeda. *Chem. Asian J.,* 2013, **8**, 2088-2095; (c) C. Qian, M. Y. Liu, G. H. Hong, P. C. Xue, P. Gong, R. Lu. *Org. Biomol. Chem.,* 2015, **13**, 2986-2998.
14 (a) S. S. Babu, V. K. Praveen, A. Ajayaghosh. *Chem. Rev.,* 2014, **114**, 1973-2129; (b) C. D. Dou, L. Han, S. S. Zhao, H. Y. Zhang, Y. Wang. *J. Phys. Chem. Lett.*, 2011, **2**, 666-670; (c) X. Q. Zhang, Z. G. Chi, J. Y. Zhang, H. Y. Li, B. J. Xu, X. F. Li, S. W. Liu, Y. Zhang, J. R. Xu. *J. Phys. Chem. B*., 2011, **115**, 7606-7611; (d) Y. Xiong, X. L. Yan, Y. W. Ma, Y. L, G. H. Yin, L. G. Chen. *Chem. Commun*., 2015, **51**, 3403-3406.
15 (a) A. Ajayaghosh, V. K. Praveen. *Acc. Chem. Res.,* 2007, **40**, 644-656; (b) M. George, R. G. Weiss. *Acc. Chem. Res.*, 2006, **39**, 489-497.
16 (a) L. Wang, Q. Su, Q. L. Wu, W. Gao, Y. Mu. *C. R. Chimie.,* 2012, **15**, 463-470; (b) S. Range, D. F. J. Piesik, S. Harder. *Eur. J. Inorg. Chem.,* 2008, 3442-3451.
17 K. Sugiyasu, N. Fujita, S. Shinkai. *Angew. Chem.*, 2004, **116**, 1249-1249.
18 (a) X. D. Yu, L. M. Chen, M. M. Zhang, T. Yi. *Chem. Soc. Rev.*, 2014, **43**, 5346-5371; (b) C. G. Pappas, P. W. J. M. Frederix, T. Mutasa, S. Fleming, Y. M. Abul-Haija, S. M. Kelly, A. Gachagan, D. Kalafatovic, J. Trevino, R. V. Ulijn, S. Bai. *Chem. Commun.*, 2015, **51**, 8465-8468.
19 M. Pandeeswar, H. Khare, S. Ramakumarb, T. Govindaraju. *Chem. Commun.*, 2015, **51**, 8315-8318.
20 M. M. Su, H. K. Yang, L. J. Ren, P. Zheng, W. Wang. Soft Matter., 2015, **11**, 741-748.
21 Y Cui, Y. M Yin, H. T Cao, M Zhang, G. G Shan, H. Z Sun, Y Wu, Z. M Su, W. F Xie. *Dyes Pigments*., 2015, **119**, 62-69.
22 J. X. Wu, H. L. Wang, S. P. Xu, W. Q. Xu. *J. Phys. Chem. A.* 2015, **119**, 1303-1308.
23 Q. B. Song, K. Chen, J. W. Sun, Y. S. Wang, M. Ouyang, C. Zhang. *Tetrahedron Lett*., 2014, **55**, 3200-3205.
24 M. Zheng, D. T. Zhang, M. X. Sun, Y. P. Li, T. L. Liu, S. F. Xue, W. J. Yang. *J. Mater. Chem. C.*, 2014, **2**, 1913-1920.
25 D. T. Zhang, Y. Y. Gao, J. Dong, Q. K. Sun,W. Liu, S. F. Xue,W. J. Yang. *Dyes Pigments*., 2015, **113**, 307-311.
26 Gaussian 09, Revision A.02, M. J. Frisch, G. W. Trucks, H. B. Schlegel, G. E. Scuseria, M. A. Robb, J. R. Cheeseman, G. Scalmani, V Barone, B Mennucci, G. A Petersson, H Nakatsuji, M. Caricato, X. Li, H. P. Hratchian, A. F. Izmaylov, J. Bloino, G. Zheng, J. L. Sonnenberg, M. Hada, M. Ehara, K. Toyota, R. Fukuda, J. Hasegawa, M. Ishida, T. Nakajima, Y. Honda, O. Kitao, H. Nakai, T. Vreven, J. A. Montgomery, Jr., J. E. Peralta, F. Ogliaro, M. Bearpark, J. J. Heyd, E. Brothers, K. N. Kudin, V. N. Staroverov, R. Kobayashi, J. Normand, K. Raghavachari, A. Rendell, J. C. Burant, S. S. Iyengar, J. Tomasi, M. Cossi, N. Rega, J. M. Millam, M. Klene, J. E. Knox, J. B. Cross, V. Bakken, C. Adamo, J. Jaramillo, R. Gomperts, R. E. Stratmann, O. Yazyev, A. J. Austin, R. Cammi, C. Pomelli, J. W. Ochterski, R. L. Martin, K. Morokuma, V. G. Zakrzewski, G. A. Voth, P. Salvador, J. J. Dannenberg, S. Dapprich, A. D. Daniels, Ö. Farkas, J. B. Foresman, J. V. Ortiz, J. Cioslowski, D. J. Fox, Gaussian, Inc., Wallingford CT, 2009.

TOC For:

Salicylaldimine Difluoroboron Complexes Containing *tert*-Butyl Groups: Nontraditional π-Gelator and Piezofluorochromic Compounds

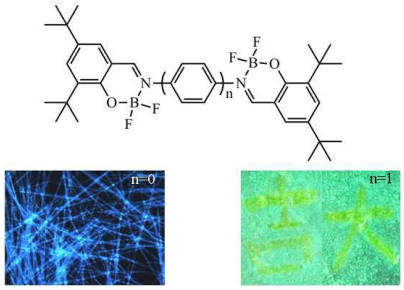

Tert-butyl can lead to the loose packing of salicylaldehydehydrazone difluoroboron complexes in aggregated states to generate stimuli-responsive materials.